Pressure-induced shift and broadening of 1560−1630-nm carbon monoxide wavelength-calibration lines

W. C. Swann and S. L. Gilbert

Optoelectronics Division, National Institute of Standards and Technology, Boulder, Colorado 80305

We have measured the line centers and the pressure-induced shifts of 14 lines in the 3ν rotational–vibrational band of carbon monoxide, $^{12}C^{16}O$, and 18 lines in the corresponding band of $^{13}C^{16}O$. These lines can be used as wavelength references in the optical fiber communication wavelength-division multiplexing L band (approximately 1565–1625 nm). The $^{12}C^{16}O$ spectrum has useful reference lines from 1560 to 1595 nm, and the $^{13}C^{16}O$ spectrum has lines from 1595 to 1630 nm. We observed that, except for a shift of 35 nm toward longer wavelengths for the $^{13}C^{16}O$ spectrum, the behaviors of the two isotopic species are similar. We found that the pressure shift varies with line number, from $\sim +0.01$ to $+0.02$ pm/kPa (~ 0.16 to 0.31 MHz/Torr). In addition, we measured the pressure broadening of these lines; we found that it also varies with line number and is typically 0.3–0.4 pm/kPa (approximately 5–7 MHz/Torr).

OCIS codes: 020.3690, 060.2330, 120.3940, 120.4800, 300.0300, 300.6390.

1. INTRODUCTION

Wavelength-division multiplexing (WDM) in optical fiber communication systems increases bandwidth by using many wavelength channels. Current WDM systems typically employ 50- or 100-GHz channel spacing (0.4 or 0.8 nm, respectively) in the 1540–1560 nm WDM C band. WDM will expand into the L-band region (approximately 1565–1625 nm) in the near future, and WDM may be implemented in shorter wavelength regions as well. Wavelength references are needed in these regions for calibration of instruments that are used to characterize components and monitor the wavelengths of the channels.

Fundamental atomic or molecular absorptions provide wavelength references that are stable under changing environmental conditions such as temperature and pressure variations or the presence of electromagnetic fields. The National Institute of Standards and Technology has developed wavelength calibration transfer standards for the 1510–1560-nm region based on acetylene and hydrogen cyanide.[1–3] We examined a number of molecules as potential references for the WDM L-band region. Hydrogen and deuterium halides generally have strong lines and simple spectra, but of these only hydrogen iodide[4] has spectral lines in the L band. Unfortunately, hydrogen iodide has several drawbacks: the spectrum (lines from 1534 to 1595 nm) only partially covers the L band, some of the lines have significant substructure owing to the electric-quadrupole hyperfine interaction, and the gas is difficult to work with because of its reactivity and tendency to decompose. We also investigated various hydrocarbons, halogenated hydrocarbons, and other gases containing one or more C—H bonds, because overtones of the C—H bond's fundamental vibrational frequency have spectra near 1550 nm. Although some of the spectra were in the correct location, we found that they either were too weak or were highly convoluted, containing hundreds of overlapping lines. These are typically not simple linear molecules, and off-axis vibrations cause complicated spectra. The carbon monoxide 3ν rotational–vibrational band has a simple spectrum in this region, but the absorption strength is small; at a pressure of 133 kPa (1000 Torr), a path length of 80 cm produces an absorption of $\sim 15\%$ for the stronger lines.

We decided to develop National Institute of Standards and Technology Standard Reference Material (SRM) transfer standards for the WDM L band based on the absorption lines of carbon monoxide ($^{12}C^{16}O$ and $^{13}C^{16}O$). Figure 1 shows the spectra for these two isotopic species; $^{12}C^{16}O$ has ~ 40 lines from 1560 to 1595 nm, and $^{13}C^{16}O$ has ~ 40 lines from 1595 to 1630 nm. The vacuum wavelengths of selected $^{12}C^{16}O$ line centers of the 3ν band have been measured and tabulated for low-pressure conditions,[5,6] with one author quoting an uncertainty of 8×10^{-6} nm.[5] Similarly accurate measurements of the corresponding band of $^{13}C^{16}O$ have not been made, to our knowledge. However, the predicted low-pressure line centers for $^{13}C^{16}O$, calculated by use of mass-independent Dunham parameters, are reported in the HITRAN database.[7] For wavelength calibration of instruments it is often desirable to use an intermediate- or high-pressure sample to pressure broaden the lines and match the reference bandwidth to the instrument resolution. Doing so results in the strongest signals for a given resolution bandwidth. To provide maximum sensitivity when it is used with a 0.05-nm resolution instrument, such as an optical spectrum analyzer, the gas in the carbon monoxide SRM will be at a pressure of ~ 133 kPa (1000 Torr). In addition to broadening the lines, the higher pressure also slightly shifts the line centers. This shift, which results from energy-level shifts caused by the interaction of mol-
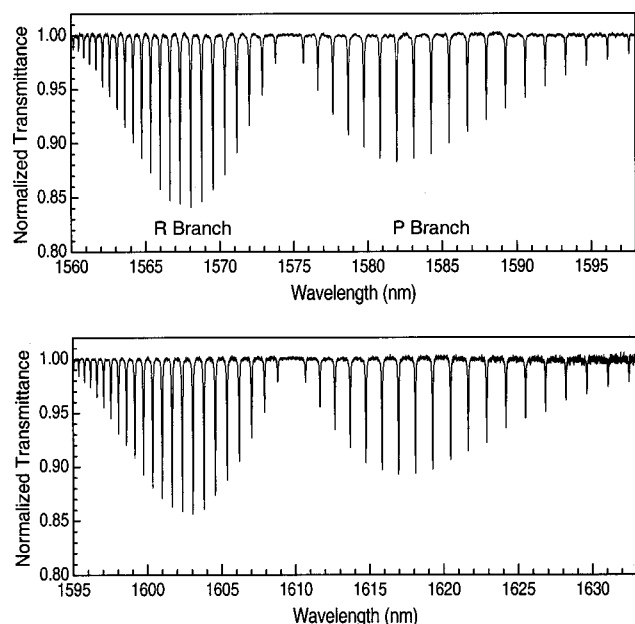
Fig. 1.   Carbon monoxide 3ν rotational–vibrational spectra. Top, the $^{12}C^{16}O$ spectrum; bottom, the $^{13}C^{16}O$ spectrum. We took these data by passing LED light through an absorption cell and recording the spectrum of the transmitted light with an optical spectrum analyzer with a 0.05-nm resolution bandwidth. The recorded spectrum divided by the LED spectrum is shown. The CO gas pressure was 133 kPa (1000 Torr); light made four passes through the cell for a total optical path length of 80 cm. The bottom spectrum is noisier because of lower power from the LED.

ecules during collisions,[8] increases linearly with pressure and is often called the pressure shift. Inasmuch as our goal is to certify the SRM references with an uncertainty of less than 1 pm, we need an accurate measurement of the pressure shift for both isotopic species. Picque and Guelachvili[5] measured the pressure shifts of a number of $^{12}C^{16}O$ lines with an uncertainty of $\sim 2.5 \times 10^{-3}$ pm/kPa, and Henningsen et al.[6] measured the pressure shift of many lines of the $^{12}C^{16}O$ R branch with an uncertainty of $\sim 1.4 \times 10^{-3}$ pm/kPa (Henningsen did not report values for the P branch). To our knowledge there are no measurements of the pressure shift of $^{13}C^{16}O$ absorption lines reported in the literature.

We measured the line centers, pressure shifts, and pressure broadening of 14 lines in the $^{12}C^{16}O$ spectrum and of 18 lines in the $^{13}C^{16}O$ spectrum. As a check on our measurement accuracy we also extrapolated these line centers to zero pressure and compared those values with the literature values. We describe our measurement procedure in Section 2 and summarize the results in Section 3. Conclusions are presented in Section 4.

2.   MEASUREMENT DESCRIPTION AND DATA ANALYSIS

A schematic diagram of our pressure-shift measurement apparatus is shown in Fig. 2. Light from a tunable diode laser is sent through two absorption cells simultaneously, and the transmission through each cell is monitored by detectors. One cell contained carbon monoxide gas (ei-

ther $^{12}C^{16}O$ or $^{13}C^{16}O$) at a relatively low pressure of ~ 27 kPa (~ 200 Torr), and the other contained the same isotopic species at a higher pressure of ~ 133 kPa (~ 1000 Torr). A third detector monitored the laser power, and a wavelength meter measured the laser's wavelength with an uncertainty of 1 part in 10^7 (0.16 pm at 1600 nm). A computer controlled the laser wavelength scan and recorded the readings of the three detectors and the wavelength meter.

Figure 3 shows spectra of line $R7$ of $^{13}C^{16}O$ obtained with the low- and high-pressure cells. The pressure broadening in the high-pressure spectrum is obvious. We are interested primarily in the shift of the high-pressure line center relative to the low-pressure line center. Fourteen lines in the $^{12}C^{16}O$ spectrum and eighteen lines in the $^{13}C^{16}O$ spectrum were scanned with this technique. The measured quantity, transmitted power I_T, is related to absorption coefficient α and absorption path length L by

$$I_T = I_0 \exp(-\alpha L), \tag{1}$$

where I_0 is the incident power. We first divided the cell transmission curves by the laser power monitor signal to
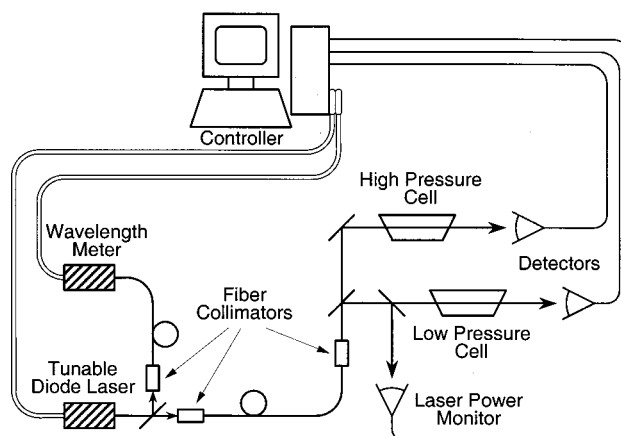

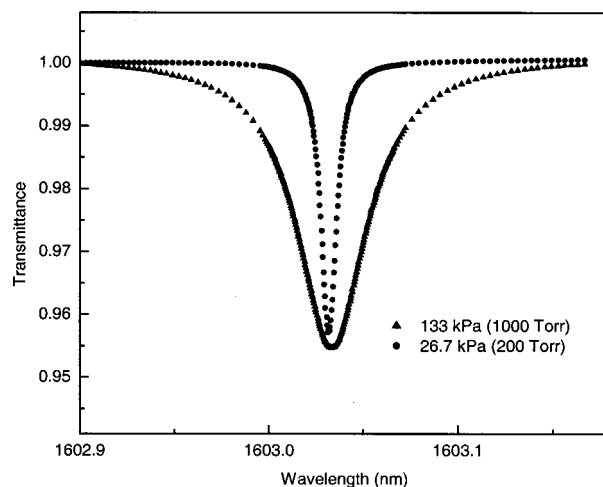Fig. 2.   Diagram of pressure-shift measurement apparatus.

Fig. 3.   Tunable diode laser scan of the $^{13}C^{16}O$ $R7$ line showing transmittance through the low-pressure (26.7-kPa) and high-pressure (133-kPa) cells.

remove common-mode intensity variations and normalized the data. We then took the natural logarithm to obtain the absorbance, αL.

Individual lines were then fitted to Voigt profiles[8] by use of an orthogonal distance regression algorithm.[9] The orthogonal distance regression, called either error-in-variables or total-least-squares regression, obtains the model parameters by minimizing the sum of squares of the orthogonal distances from the model to the data points. The fitting program was able to account for a background slope and uncertainties in both x (wavelength) and y (transmitted power). A Voigt profile is a convolution of Lorentzian and Gaussian profiles; it results when there is a combination of Gaussian broadening (resulting from Doppler broadening, for example) and Lorentzian line shape (resulting from the natural linewidth or pressure broadening, for example). In our situation, the natural linewidth is small (typically <2 MHz for molecular absorption lines in this region[10]) compared with the Gaussian Doppler broadening (~400 MHz) and the Lorentzian pressure broadening. The pressure-broadened component of the linewidths ranged from 2× to 55× the Doppler-broadened component. We fixed the Doppler linewidth at 3.65 pm (Ref. 8) and allowed other fitting parameters to vary.

The fused-silica absorption cells are 20 cm long, with windows attached to the cells by a glass frit method. To prevent interference fringes in the transmitted signal the windows are mounted at an angle of 11° and also are wedged by ~2°. The cells were first evacuated and leak checked and were then filled with isotopically pure gas (99.95% $^{12}C^{16}O$ or 99% $^{13}C^{16}O$). During the fill process the pressure in the fill manifold (and hence in the cell) was monitored with a capacitance manometer. Once filled, the cells were closed off with a glass valve with O-ring seals. To check a cell's pressure after closing the valve (which changes the cell's pressure as the valve's O ring compresses), and to monitor a cell's pressure over the course of the measurements, we generated a plot of the Lorentzian component of the linewidth (derived from the Voigt line fit) versus pressure for line $R7$. This allowed us to determine a cell's pressure at any time by measuring the width of line $R7$ and comparing it with the plot. To generate the plot we mounted a cell in our pressure-shift measurement apparatus and attached it to our fill manifold with a copper tube. In this way we monitored the cell pressure by using the capacitance manometer while we measured the linewidth and the line center. We conducted these measurements on line $R7$ of both isotopic species for several pressures from 13.3 kPa (100 Torr) to 133 kPa (1000 Torr). Figure 4(a) is a plot of the full width at half-maximum (FWHM) of the Lorentzian component of the $^{13}C^{16}O$ line $R7$ versus pressure and a linear least-squares fit to the data. As can be seen from the figure, the Lorentzian component of the width (pressure broadening) has a linear dependence on pressure. Figure 4(b) shows the line-center wavelength versus pressure of the same line and the corresponding linear least-squares fit; as can be seen from this figure, the pressure shift is also linearly dependent on pressure. Based on our calibration of linewidth versus pressure for line $R7$, the pressures for the low- and high-pressure cell pairs
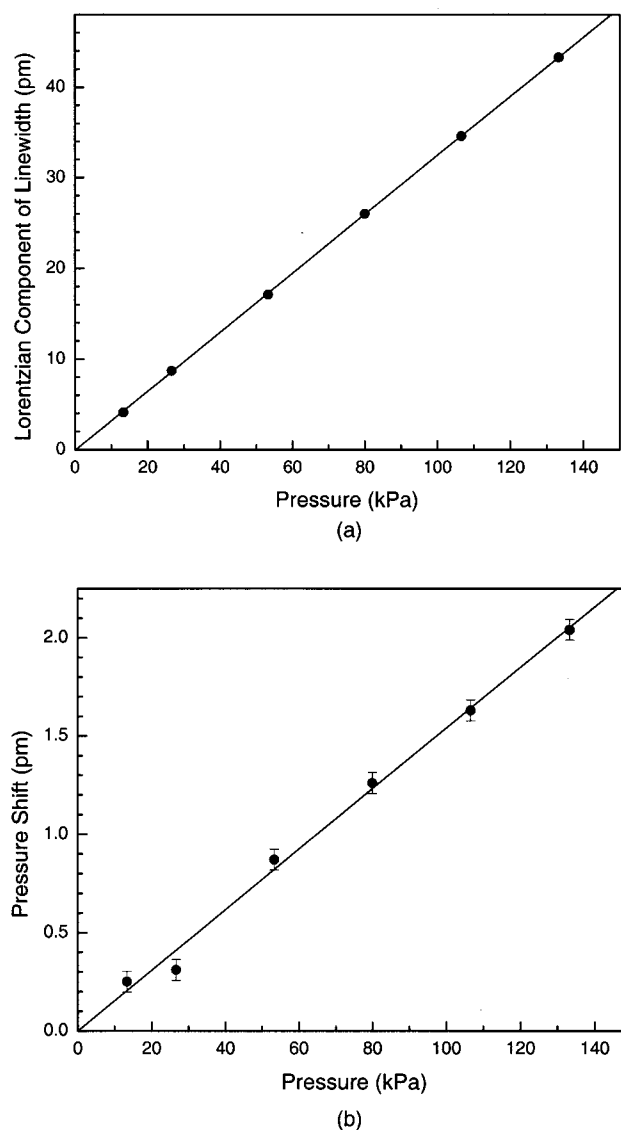

Fig. 4. (a) FWHM of the Lorentzian component of the $^{13}C^{16}O$ $R7$ line versus pressure and the corresponding linear least-squares fit to the data (error bars are smaller than the points). (b) Line $R7$ center wavelength shift from the zero-pressure value versus pressure and the corresponding linear least-squares fit to the data; the error bars are 1 standard uncertainty (1σ).

used in the subsequent shift measurements were 26.4 ± 0.5 kPa (198 ± 4 Torr) and 134.5 ± 1.3 kPa (1009 ± 10 Torr) for $^{12}C^{16}O$, and 26.9 ± 0.5 kPa (202 ± 4 Torr) and 133.5 ± 1.3 kPa (1001 ± 10 Torr) for $^{13}C^{16}O$. The pressure uncertainty quoted here is the expanded uncertainty that we obtained by applying a coverage factor $k = 2$ (i.e., our quoted uncertainty is ±2σ).[11]

Inasmuch as the spectra for the low- and high-pressure cells were measured simultaneously, the absolute accuracy of the wavelength meter was not of critical importance for measurement of the relative pressure shift. However, the short-term statistical variation of the wavelength measurement did add noise to the data. To determine this statistical variation we repeatedly measured a laser that was stabilized to a narrow rubidium line. The statistical variation of repeated measurements yielded a Gaussian distribution with a standard deviation of 0.1

pm. Because of the band coverage of the two carbon monoxide spectra, and the band limitations of our lasers, we needed to use two different lasers through the course of the measurement. We determined the experimental uncertainty in the signal level by measuring the statistical variation of the data within a region of a line wing. The standard deviation of the fluctuations was 3 parts in 10^5 and 8 parts in 10^6 of the transmitted power, depending on the laser used.

Each data point was assigned a standard uncertainty of 0.1 pm for the wavelength and a fractional uncertainty of 3 parts in 10^5 or 8 parts in 10^6, depending on which laser we used, for the transmitted power. The fitting program determined the line centers and the Lorentzian component of the linewidths, the corresponding uncertainties, and the reduced residual-sum-of-squares (χ^2) value for the fit.

A. Background Variation

A slope or a variation in the background level can shift the apparent center of a line, particularly for the wide lines of the high-pressure cells. Nearby absorption lines, interference fringes owing to reflected laser light, wavelength dependence of the optical components, beam pointing stability, and variations in the laser power can cause background variation. We found no evidence of nearby absorption lines in either spectrum. As mentioned above, we removed common-mode laser power variations by dividing the cell transmittance data by the power monitor data. Owing to the wavelength dependence of optical fiber couplers (splitters), we used free-space beam splitters to send the laser light to the cells and the power monitor. We minimized interference effects by using wedged cell windows and beam splitters, windowless detectors, and two optical isolators.

Because the remaining background variations were not purely statistical noise, they can potentially add uncertainty to our measurements. We modeled the effect of these variations to determine their contribution to our line-center and linewidth uncertainties. Two model Voigt functions were generated to represent the strongest ($R7$) and the weakest ($P19$) lines that we measured in $^{13}C^{16}O$. We obtained a sample baseline spectrum by scanning a cell transmittance in a spectral region between two absorption lines. Sections of this baseline noise were then added to the model lines, along with modeled wavelength measurement noise. The resultant noisy modeled lines were then fitted by the procedure described above. We then repeated this process approximately 25 times, using a different sample of baseline noise each time; this resulted in a set of fit parameters for the centers and widths of both lines. For the weaker line we found that the standard deviations of the line-fitting parameters were considerably larger than the uncertainties returned by the fitting program for a single line fit (0.09 versus 0.03 pm for the line center and 0.6 versus 0.2 pm for the linewidth of the high-pressure sample). For the stronger line, however, the standard deviations of the modeled line-fitting parameters were approximately the same as the uncertainties returned by the fitting program for a single line fit. This result is not surprising, because we would expect the background noise to have a larger effect for the weaker line. To verify the results of the model we scanned and fitted lines $R7$ and $P19$ eleven times. The standard deviation of the fit parameters agreed with our simulation results. To account for the effect of background variations on the other lines' uncertainties, we interpolated the results that we obtained for lines $P19$ and $R7$ to the other lines based on their line strength.

B. Wavelength Accuracy

Although the absolute accuracy of the wavelength measurement was not relevant to the pressure-shift measurement, extrapolating our line-center measurements to zero pressure and comparing them with literature values serves as a good verification of our measurements. To determine the line-center accuracy for our measurements we first checked the accuracy of the wavelength meter used in the measurements. We set up a high-accuracy wavelength reference for this purpose.[3] Diode laser light at 1560.5 nm was amplified with an erbium-doped fiber amplifier and was frequency doubled in a periodically poled lithium niobate crystal. The resultant 780-nm light was then used to conduct saturated absorption spectroscopy on the $5S_{1/2} \to 5P_{3/2}$ transitions of rubidium (^{85}Rb and ^{87}Rb). The line centers of the hyperfine components of these transitions have been measured with an uncertainty of ±0.4 MHz (Ref. 12); a subset of these lines has been measured to higher accuracy.[13] We stabilized the laser to several different hyperfine components of the ^{87}Rb transition and compared the wavelength meter reading (vacuum wavelength) with the literature values multiplied by 2. As the lines were very narrow (less than 10 MHz), the absolute stability of the laser was much better than the quoted wavelength meter uncertainty of 1 part in 10^7 ($\sim$20 MHz at 1600 nm). From measurements taken before and after our pressure-shift scans we found that the wavelength meter reading was offset by -0.07 ± 0.07 pm ($+9 \pm 9$ MHz). The uncertainty (2σ) is derived from the standard deviation of multiple wavelength meter calibration measurements made over the course of the pressure-shift measurement. During this time the wavelength meter's offset varied from $+0.03$ pm to -0.13 pm.

3. PRESSURE SHIFT, LINE CENTER, AND PRESSURE-BROADENING RESULTS

Tables 1 and 2 summarize our line-center, pressure-shift, and pressure-broadening results. To obtain the unperturbed line-center values we adjusted the low- and high-pressure line-center data for the wavelength meter's offset and extrapolated the line centers to zero pressure by use of a Monte Carlo fitting procedure. We also derived the pressure-shift coefficient (change in line-center wavelength versus pressure) from this Monte Carlo fit. The pressure-broadening coefficient for each line was determined by a Monte Carlo fit to the Lorentzian component of the high- and low-pressure linewidths.

Temperature changes can slightly modify the pressure shift and pressure broadening of a molecular line by changing the collision frequency.[8] For the measurements reported here, the temperature was 22 ± 2 °C. As discussed in Ref. 1, this temperature range would cause a

Table 1. $^{12}C^{16}O$ Line-Center, Pressure-Shift, and Pressure-Broadening Results[a]

Line	Line Center Extrapolated to Zero Pressure (nm)	Shift Coefficient		Broadening Coefficient	
		pm/kPa	MHz/Torr	pm/kPa	MHz/Torr
$R21$	1560.50004(24)	0.0188(20)	−0.309(32)	0.267(14)	4.38(22)
$R16$	1562.59327(20)	0.0157(18)	−0.257(29)	0.273(12)	4.47(20)
$R12$	1564.74563(14)	0.0154(8)	−0.251(13)	0.294(8)	4.80(14)
$R7$	1568.03555(10)	0.0147(6)	−0.239(10)	0.315(6)	5.12(10)
$R4$	1570.33051(14)	0.0131(10)	−0.212(16)	0.339(8)	5.49(12)
$R1$	1572.86770(20)	0.0109(16)	−0.176(26)	0.388(12)	6.27(20)
$R0$	1573.76745(24)	0.0097(20)	−0.157(32)	0.407(14)	6.57(22)
$P1$	1575.64836(24)	0.0112(20)	−0.180(32)	0.413(14)	6.65(22)
$P2$	1576.62961(20)	0.0115(18)	−0.185(29)	0.385(12)	6.19(20)
$P4$	1578.67400(16)	0.0139(14)	−0.223(22)	0.359(12)	5.76(20)
$P7$	1581.94641(16)	0.0159(10)	−0.254(16)	0.330(8)	5.27(12)
$P11$	1586.69708(16)	0.0172(14)	−0.273(22)	0.312(8)	4.95(12)
$P15$	1591.89544(20)	0.0182(18)	−0.285(28)	0.295(12)	4.65(18)
$P19$	1597.54775(24)	0.0191(20)	−0.299(31)	0.279(14)	4.37(22)

[a] Results for the measured lines of the 3ν band of carbon monoxide $^{12}C^{16}O$ at a temperature of 22 ± 2 °C.   Line-center vacuum wavelength results are for low-pressure conditions; our measurements (column 2) are values obtained by extrapolation of the line center to zero pressure.   The broadening coefficient is the pressure dependence of the FWHM of the Lorentzian component of the Voigt line profile.   The uncertainties in the final digits of the values are indicated in parentheses.   The uncertainties quoted are the expanded uncertainties obtained by application of a coverage factor $k = 2$ (i.e., our quoted uncertainty is $\pm2\sigma$).

Table 2. $^{13}C^{16}O$ Line-Center, Pressure-Shift, and Pressure-Broadening Results[a]

Line	Line Center Extrapolated to Zero Pressure (nm)	Shift Coefficient		Broadening Coefficient	
		pm/kPa	MHz/Torr	pm/kPa	MHz/Torr
$R21$	1595.37446(20)	0.0200(20)	−0.314(38)	0.253(16)	3.97(26)
$R18$	1596.58693(20)	0.0187(20)	−0.293(34)	0.272(16)	4.27(25)
$R15$	1598.03287(18)	0.0160(18)	−0.250(28)	0.287(12)	4.50(20)
$R12$	1599.71196(16)	0.0160(12)	−0.250(20)	0.303(10)	4.74(15)
$R10$	1600.96157(16)	0.0152(12)	−0.237(18)	0.313(8)	4.88(13)
$R7$	1603.03136(12)	0.0152(8)	−0.237(14)	0.326(8)	5.07(12)
$R4$	1605.33673(16)	0.0134(12)	−0.208(20)	0.345(10)	5.36(16)
$R1$	1607.87857(20)	0.0106(20)	−0.164(32)	0.401(14)	6.20(22)
$R0$	1608.77849(20)	0.0101(20)	−0.157(38)	0.419(16)	6.47(26)
$P1$	1610.65814(20)	0.0111(20)	−0.171(36)	0.424(16)	6.54(24)
$P2$	1611.63775(20)	0.0118(20)	−0.182(32)	0.410(14)	6.31(22)
$P4$	1613.67706(18)	0.0136(16)	−0.209(26)	0.368(14)	5.65(21)
$P7$	1616.93687(16)	0.0167(14)	−0.255(20)	0.342(10)	5.23(16)
$P9$	1619.24491(16)	0.0171(14)	−0.261(22)	0.329(10)	5.02(16)
$P11$	1621.66151(18)	0.0184(14)	−0.280(22)	0.320(10)	4.87(15)
$P13$	1624.18751(18)	0.0175(16)	−0.265(24)	0.318(12)	4.82(18)
$P16$	1628.18261(20)	0.0191(20)	−0.288(34)	0.300(16)	4.52(22)
$P19$	1632.42759(20)	0.0209(20)	−0.314(36)	0.286(16)	4.29(24)

[a] Results for the measured lines of the 3ν band of carbon monoxide $^{13}C^{16}O$ at a temperature of 22 ± 2 °C.   Line center-vacuum wavelength results are for low-pressure conditions; our measurements (column 2) are values obtained by extrapolation of the line center to zero pressure.   The broadening coefficient is the pressure dependence of the FWHM of the Lorentzian component of the Voigt line profile.   The uncertainties in the final digits of the values are indicated in parentheses.   The uncertainties quoted are the expanded uncertainties obtained by application of a coverage factor $k = 2$ (i.e., our quoted uncertainty is $\pm2\sigma$).

$\pm0.3\%$ change in the pressure shift and pressure broadening, which is negligible compared with our pressure-shift and presure-broadening uncertainties.

Figure 5 shows the pressure shift versus line number for $^{13}C^{16}O$.   In all cases the wavelength shift was positive with increasing pressure.   The R and P branches of both isotopic species showed similar shift-versus-line number behavior, with a shift of approximately 0.01 pm/kPa for lines near the band center, rising to $\sim$0.02 pm/kPa for

lines far from the band center (i.e., transitions between states with high rotational quantum numbers).

As discussed above, pressure broadening is responsible for the Lorentzian component of the Voigt line shape.   We found that the pressure broadening also varied with line number (Fig. 6).   In contrast to the pressure-shift dependence, however, the pressure broadening was largest for lines near the band center (transitions between states with low rotational quantum numbers).   The pressure-

broadening data for $^{12}C^{16}O$ showed similar trends and magnitudes. Our pressure-broadening analysis does not include the small effect of collisional narrowing that is due to velocity averaging. This effect is negligible at higher pressures, where pressure broadening dominates, but can cause the line shape to deviate from the expected Voigt profile at low pressures.[14] Since we do not observe significant discrepancies between our data and the Voigt function, we conclude that the line-shape modification that is due to collisional narrowing is negligible at the level of our quoted uncertainty.

Figure 7 compares our $^{12}C^{16}O$ pressure-shift results with those of Picque and Guelachvili[5] and Henningsen et al.[6] Our pressure-shift standard uncertainty (1σ) ranges from 3×10^{-4} to 1×10^{-3} pm/kPa; the uncertainty quoted in Ref. 5 is 2.5×10^{-3} pm/kPa, and the uncertainty quoted in Ref. 6 is $\sim 1.4 \times 10^{-3}$ pm/kPa. Our shift values have lower uncertainty and are in good agreement with those of Refs. 5 and 6; the differences between our values and those previous measurements are within the quoted uncertainty for each line. Our pressure-broadening results also agree well with those reported in Ref. 6 for the R branch of $^{12}C^{16}O$ (Ref. 6 does not report
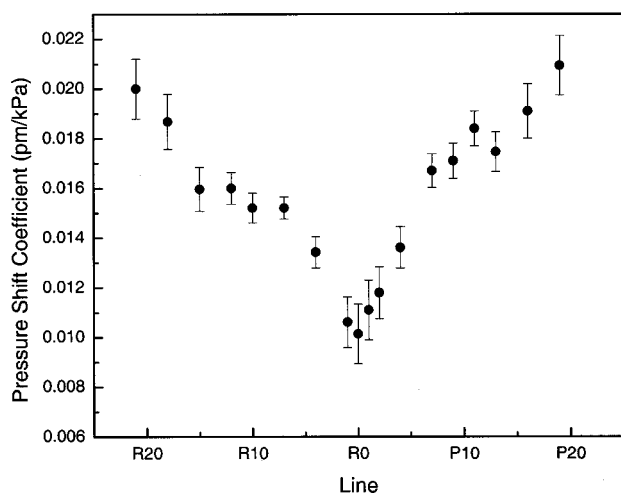

Fig. 7. Comparison of $^{12}C^{16}O$ pressure-shift results. Plotted is the difference between the results of this work, with 1σ standard uncertainty error bars, and the measurements of Picque and Guelachvili.[5] The difference between the results of Henningsen et al.[6] and Ref. 5 are also plotted.

Fig. 5. Pressure-shift coefficient versus line number for $^{13}C^{16}O$.
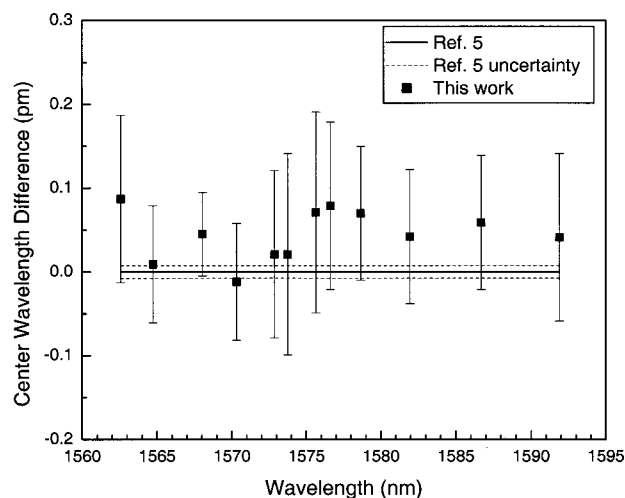
Fig. 8. Comparison of $^{12}C^{16}O$ line-center results. Plotted is the difference between the results of this work, with 1σ standard uncertainty error bars, and the measurements of Picque and Guelachvili.[5] The HITRAN database values[7] (not shown) are all within 0.02 pm of the Picque–Guelachvili values.

values in the P branch). Figure 8 compares our determinations of the zero-pressure line-center values for $^{12}C^{16}O$ with the more accurate values reported in Ref. 5, which were also extrapolated to zero pressure. Our standard uncertainty (1σ) is typically near 0.1 pm, whereas the estimated uncertainty given in Ref. 5 is 3×10^{-5} cm^{-1} (0.008 pm). All our line-center values are in good agreement with those of Refs. 5 and 7; the differences between the values are within our standard uncertainty for each line center. To date, the only reference that we have found that reports zero-pressure line-center values for $^{13}C^{16}O$ is the HITRAN database.[7] To our knowledge, there are no measurements of the pressure shift of $^{13}C^{16}O$ absorption lines reported in the literature. Our zero-pressure line-center values for $^{13}C^{16}O$ are in good agreement with the HITRAN values; the differences between our values and the HITRAN values are less than 0.15 pm. These comparisons with calculations and previous mea-
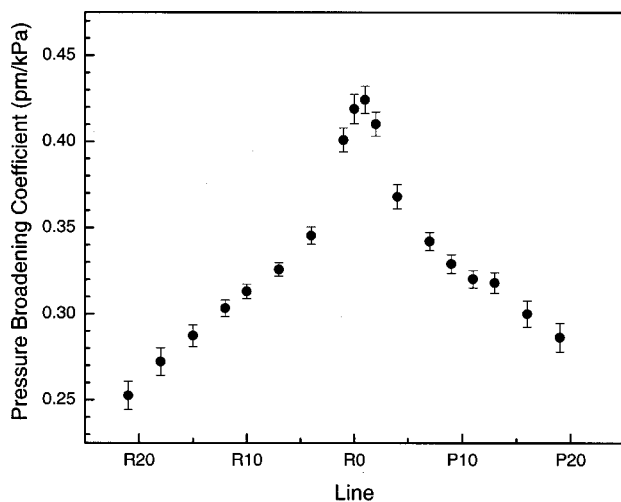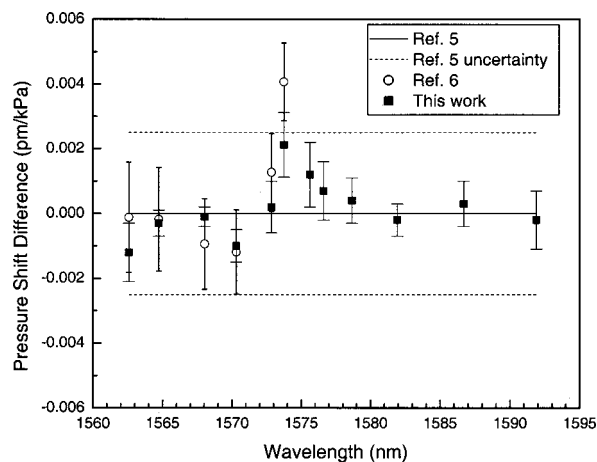

Fig. 6. Pressure dependence of the Lorentzian component (FWHM) of the linewidth versus line number for $^{13}C^{16}O$.

surements give us further confidence in our analysis of the pressure-shift coefficient values and uncertainties for the $^{12}C^{16}O$ and $^{13}C^{16}O$ measurements.

4. CONCLUSIONS

We have measured the pressure-shift coefficient for 14 lines of the $^{12}C^{16}O$ isotopic species and 18 lines of the $^{13}C^{16}O$ isotopic species of the 3ν rotational–vibrational band of carbon monoxide. The two isotopic species showed nearly identical shift behavior, with a shift of $\sim +0.01$ pm/kPa (equivalently, $+1.3 \times 10^{-3}$ pm/Torr or -0.16 MHz/Torr) near the band center and of ~ 0.02 pm/kPa (equivalently, $+2.7 \times 10^{-3}$ pm/Torr or -0.31 MHz/Torr) for lines farther from the band center. We have also measured the pressure broadening of these lines and found that it also varies with line number, ranging from 0.25 pm/kPa (4 MHz/Torr) to 0.42 pm/kPa (6.5 MHz/Torr). For a pressure of 133 kPa ($\sim$1000 Torr; the conditions of the National Institute of Standards and Technology SRM) the pressure shift is typically near 2 pm but can be as large as 2.8 pm for lines far from the band center and as low as 1.3 pm for lines near the band center. The Lorentzian component of the linewidths at this pressure varies from 34 pm ($\sim$4 GHz) for lines far from the band center to 56 pm ($\sim$7 GHz) near the band center.

Although the pressure shift and the pressure broadening are both due to the interactions between molecules during collisions, they depend on line number rather differently. The pressure shift is largest for lines far from the band center (transitions between states with high rotational quantum number J), whereas the pressure broadening is largest for lines near the band center (transitions between states with low J). One explanation for the pressure-broadening line dependence is that rotational averaging of the potential during a collision causes states with high rotational angular momentum (high J) to be perturbed less than states with low J. The pressure shift is more difficult to interpret; it represents the difference between the shift of the excited state and the shift of the ground state. We would need to conduct a more extensive study before drawing any conclusions about the shift of a particular state. Our measurements of pressure broadening and shift of acetylene lines[1] show trends that are similar to those observed in carbon monoxide.

ACKNOWLEDGMENTS

S. L. Gilbert can be reached by e-mail at sgilbert @boulder.nist.gov.

REFERENCES

1. W. C. Swann and S. L. Gilbert, "Pressure-induced shift and broadening of 1510–1540-nm acetylene wavelength calibration lines," J. Opt. Soc. Am. B **17**, 1263–1270 (2000).
2. S. L. Gilbert and W. C. Swann, "Acetylene $^{12}C_2H_2$ absorption reference for 1510 nm to 1540 nm wavelength calibration—SRM 2517a," Natl. Inst. Stand. Technol. (US) Spec. Publ. **260−133** (2001).
3. S. L. Gilbert, W. C. Swann, and C. M. Wang, "Hydrogen cyanide $H^{13}C^{14}N$ absorption reference for 1530–1560 nm wavelength calibration—SRM 2519," Natl. Inst. Stand. Technol. (US) Spec. Publ. **260−137** (1998).
4. F. Bertinetto, P. Gambini, R. Lano, and M. Puleo, "Stabilization of the emission frequency of 1.54 μm DFB laser diodes to hydrogen iodide," IEEE Photon. Technol. Lett. **4**, 472–474 (1993).
5. N. Picque and G. Guelachvili, "Absolute wavenumbers and self-induced pressure lineshift coefficients for the 3–0 vibration–rotation band of $^{12}C^{16}O$," J. Mol. Spectrosc. **185**, 244–248 (1997).
6. J. Henningsen, H. Simonsen, T. Møgelberg, and E. Trudsø, "The $0 \rightarrow 3$ overtone band of CO: precise linestrengths and broadening parameters," J. Mol. Spectrosc. **193**, 354–362 (1999).
7. L. S. Rothman, C. P. Rinsland, A. Goldman, S. T. Massie, D. P. Edwards, J.-M. Flaud, A. Perrin, C. Camy-Peyret, V. Dana, J.-Y. Mandin, J. Schroeder, A. McCann, R. R. Gamache, R. B. Wattson, K. Yoshino, K. V. Chance, K. W. Jucks, L. R. Brown, V. Nemtchinov, and P. Varanasi, "The HITRAN molecular spectroscopic database and HAWKS (HITRAN atmospheric workstation): 1996 edition," J. Quant. Spectrosc. Radiat. Transfer **60**, 665–710 (1998); http://www.hitran.com
8. W. Demtröder, *Laser Spectroscopy*, 2nd ed. (Springer-Verlag, Berlin, 1996), pp. 67–82.
9. P. A. Boggs, R. H. Byrd, J. E. Rogers, and R. B. Schnabel, "Users reference guide for ODRPAC version 2.01 software for weighted orthogonal distance regression," Natl. Inst. Stand. Technol. (US) Interagency Rep. **4834** (1992).
10. K. Nakagawa, M. de Labachelerie, Y. Awaji, and M. Kourogi, "Accurate optical frequency atlas of the 1.5-μm bands of acetylene," J. Opt. Soc. Am. B **13**, 2708–2714 (1996).
11. B. N. Taylor and C. E. Kuyatt, "Guidelines for evaluating and expressing the uncertainty of NIST measurement results," Natl. Inst. Stand. Technol. (US) Tech. Note **1297** (1993).
12. G. P. Barwood, P. Gill, and W. R. C. Rowley, "Frequency measurements on optically narrowed Rb-stabilized laser diodes at 780 nm and 795 nm," Appl. Phys. B **53**, 142–147 (1991).
13. J. Ye, S. Swartz, P. Jungner, and J. Hall, "Hyperfine structure and absolute frequency of the ^{87}Rb $5P_{3/2}$ state," Opt. Lett. **21**, 1280–1282 (1996).
14. P. L. Varghese and R. K. Hanson, "Collisional narrowing effects on spectral line shapes measured at high resolution," Appl. Opt. **23**, 2376–2385 (1984).